

FINITE ELEMENT SIMULATIONS OF ELASTO-VISCOPLASTIC STEADY FLOWS WITHIN A LID-DRIVEN CAVITY

Renato Martins, renato@mecanica.ufrgs.br

Giovanni Minervino Furtado, giovannimf@mecanica.ufrgs.br

Daniel Dall'Onder dos Santos, dallonder@mecanica.ufrgs.br

Sérgio Frey, frey@mecanica.ufrgs.br

Laboratory of Computational and Applied Fluid Mechanics (LAMAC) - Mechanical Engineering Department- Federal University of Rio Grande do Sul - Rua Sarmento Leite, 425 - 90050-170 – Porto Alegre, RS, Brazil

Paulo R. de Souza Mendes, pmendes@puc-rio.br

Mônica F. Naccache, naccache@puc-rio.br

Department of Mechanical Engineering, Pontifícia Universidade Católica do Rio de Janeiro
Rua Marquês de São Vicente 225, RJ 22453-900, Brazil

Abstract. *The current article aims to perform stabilized finite element approximations for inertialess flows of elasto-viscoplastic fluids. The numerical method employed to approximate the mechanical model equations is the Galerkin least-squares method, in terms of the extra-stress, pressure and velocity. This method is more stable than the classical Galerkin method, what is achieved by the addition of mesh-dependent terms, functions of the residuals of the governing equations. The simulations were performed on a lid-driven cavity employing the elasto-viscoplastic model introduced by Nassar et al., 2011. To evaluate the influence of the elasticity, power-law index and jump number, θ^* is varied from 0.2 to 2.0, n from 0.4 to 1.0 and J from 500 to 10000.*

Keywords: *elasto-viscoplasticity, stabilized Galerkin method, lid-driven cavity flow, multi-field approximation*

1. INTRODUCTION

A large variety of non-Newtonian materials exhibits a yield stress, below which they have a high viscosity or even rigid body behavior and above which they behave as a shear-thinning liquid. A list of several materials exhibiting a yield includes cement slurries, drilling muds and heavy oils in the petroleum industry; mayonnaise, butter, creams, pastes and many dairy products in the food and cosmetics industries; clay, mud and other concentrated suspensions in nature. Models have been proposed along the years to better approximate the yield-stress behavior with the experimental results, since elasticity is being also observed on these fluids. Nassar *et al.* (2011) proposed a elasto-viscoplastic model based on the Oldroyd-B fluid model which takes into account the elastic effects actually seen on many experimental results.

The main purpose of this paper is to study elasto-viscoplastic fluid flows using a multi-field Galerkin least-squares (GLS) finite element formulation which takes into account velocity, pressure and extra-stress fields as primal variables. The classical Galerkin method does not guarantee stable approximations, showing some numerical pathologies – such as the locking of the velocity field and spurious oscillations on the pressure field – when the Babuška-Brezzi finite element subspaces conditions are not satisfied. The alternative employed in this work is to enhance the Galerkin stability – adding mesh-dependent terms to the formulation – without upsetting its consistency.

The dimensionless relaxation time for elasto-viscoplastic liquids, the regularization number of the modified SMD viscosity model – namely the jump number J , introduced by Souza Mendes *et al.* (2007) – and the power-law index were ranged in order to investigate the effects of these quantities on the morphology of the unyielded zones of the flow. The numerical computations, considering steady-state creeping flows, have been carried out for power-law indexes ranging from 0.4 to 1.0, the jump number J varying from 500 to 10000 and the dimensionless relaxation time from 0.2 to 2.0. The numerical results generated by the GLS approximations were physically coherent with the flow dynamics of the problem, being in accordance with the trends pointed out on the literature.

2. MECHANICAL MODELING

The mechanical model of this work may be written coupling the momentum balance and the mass conservation equations with a modification for the upper-convected Oldroyd-B viscoelastic constitutive equation. The main goal of the elasto-viscoplastic model employed is replace the constant value viscosity, relaxation and retardation times – on the Oldroyd-B model – for expressions that are functions of the strain rate – see Nassar *et al.* (2011) for further details.

The constitutive equation for the elasto-viscoplastic model is given by:

$$\boldsymbol{\tau} + \theta_1(\dot{\gamma}) \overset{\nabla}{\boldsymbol{\tau}} = 2 \eta(\dot{\gamma}) (\mathbf{D}(\mathbf{u})) + \theta_2(\dot{\gamma}) \overset{\nabla}{\mathbf{D}}(\mathbf{u}) \quad (1)$$

where $\boldsymbol{\tau}$ is the extra stress tensor, \mathbf{D} the strain rate tensor, $\overset{\nabla}{\boldsymbol{\tau}}$ and $\overset{\nabla}{\mathbf{D}}$ represent their upper-convected derivatives, respectively given by

$$\overset{\nabla}{\boldsymbol{\tau}} = (\nabla \boldsymbol{\tau}) \mathbf{u} - (\nabla \mathbf{u}) \cdot \boldsymbol{\tau} - \boldsymbol{\tau} \cdot (\nabla \mathbf{u})^T \quad \text{and} \quad \overset{\nabla}{\mathbf{D}} = (\nabla \mathbf{D}) \mathbf{u} - (\nabla \mathbf{u}) \cdot \mathbf{D} - \mathbf{D} \cdot (\nabla \mathbf{u})^T \quad (2)$$

with the magnitude of the strain rate tensor given by $\dot{\gamma} = \sqrt{2 \operatorname{tr}[\mathbf{D}(\mathbf{u})^2]}$ and \mathbf{u} representing the velocity field.

The viscosity function employed in this work is a modification – by adding an infinite shear rate viscosity – of the expression proposed by de Souza Mendes and Dutra (2004),

$$\eta(\dot{\gamma}) = \left(1 - \exp\left(-\frac{\eta_0}{\tau_0} \dot{\gamma}\right) \right) \left(\frac{\tau_0}{\dot{\gamma}} + K \dot{\gamma}^{n-1} \right) + \eta_\infty \quad (3)$$

The relaxation and retardation times are given by the following functions:

$$\theta_1(\dot{\gamma}) = (\theta_{01} - \theta_{\infty_1}) \exp\left(-\eta_0 \dot{\gamma} / \tau_0\right) + \theta_{\infty_1} \quad (4)$$

$$\theta_2(\dot{\gamma}) = (\theta_{02} - \theta_{\infty_2}) \exp\left(-\eta_0 \dot{\gamma} / \tau_0\right) + \theta_{\infty_2} \quad (5)$$

where θ_{01} and θ_{∞_1} are, respectively, the below-yield and above-yield relaxation times; θ_{02} and θ_{∞_2} are, respectively, the below-yield and above-yield retardation times – neglected in this work. According to Eqs. (3)–(5), for the unyielded material – in the limit when $\dot{\gamma} \rightarrow 0$, $\eta(\dot{\gamma}) \rightarrow \eta_0$, $\theta_1(\dot{\gamma}) \rightarrow \theta_{01}$ and $\theta_2(\dot{\gamma}) \rightarrow \theta_{02}$ – the model tends to the classical Oldroyd-B model. On the other hand, for the yielded material – when $\dot{\gamma} > \dot{\gamma}_0$, $\eta(\dot{\gamma}) \rightarrow (\tau_0 / \dot{\gamma}) + K \dot{\gamma}^{n-1} + \eta_\infty$, $\theta_1(\dot{\gamma}) \rightarrow \theta_{\infty_1}$ and $\theta_2(\dot{\gamma}) \rightarrow \theta_{\infty_2}$ – we have an Oldroyd-B equation with a Herschel–Bulkley type viscosity, with constant relaxation and retardation times, equal to θ_{∞_1} and θ_{∞_2} , respectively. In the special case for which $\theta_{\infty_1} = \theta_{\infty_2} = 0$, the Generalized Newtonian Liquid model is recovered when $(\dot{\gamma} > \dot{\gamma}_0)$.

On Eq. (6) are summarized the mechanical model equations employed in this work, altogether with the appropriate velocity and stress boundary conditions.

$$\begin{aligned} \operatorname{div} \mathbf{u} &= 0 && \text{in } \Omega \\ \rho(\nabla \mathbf{u}) \mathbf{u} + \nabla p - \operatorname{div} \boldsymbol{\tau} - \mathbf{f} &= 0 && \text{in } \Omega \\ \boldsymbol{\tau} + \theta_1(\dot{\gamma}) \overset{\nabla}{\boldsymbol{\tau}} &= 2 \eta(\dot{\gamma}) (\mathbf{D}(\mathbf{u}) + \theta_2(\dot{\gamma}) \overset{\nabla}{\mathbf{D}}(\mathbf{u})) && \text{in } \Omega \\ \mathbf{u} &= \mathbf{u}_g && \text{on } \Gamma_g^u \\ \boldsymbol{\tau} &= \boldsymbol{\tau}_g && \text{on } \Gamma_g^\tau \\ [\boldsymbol{\tau} - p \mathbf{1}] \mathbf{n} &= \mathbf{t}_h && \text{on } \Gamma_h^\tau \end{aligned} \quad (6)$$

where ρ is the fluid density, p the hydrostatic pressure, \mathbf{f} is the body force vector; \mathbf{t}_h is the stress vector, \mathbf{u}_g and $\boldsymbol{\tau}_g$ are the imposed velocity and extra-stress boundary conditions, respectively.

2.1 Numerical approximation

To approximate the mechanical model described above it was employed a multi-field stabilized Galerkin least-squares formulation in terms of velocity, pressure and extra-stress. The classical Galerkin method does not guarantee stable approximations, may generate solutions without physical meaning and numerical pathologies for mixed incompressible fluid flows. The inherent difficulties associated to the Galerkin method are due to the compatibility of velocity and pressure finite element subspaces, e.g., the need to satisfy the Babuška-Brezzi condition involving these subspaces, a condition which was established by Babuška and Brezzi in the early 70's. The velocity and pressure subspaces may not be spanned by any arbitrary combination of finite element interpolations and, in the case of this work, which employs a multi-field formulation, another compatibility condition must be imposed on the choice of the stress and velocity subspaces. The alternative to remedy Galerkin deficiencies adopted here for incompressible fluid flows was to change the classical Galerkin formulation – adding mesh-dependent terms, which are functions of the residuals of flow governing equations, evaluated element-wise – and use simple Lagrangean elements.

3. NUMERICAL RESULTS

Figure 1 schematically shows the $L_c \times L_c$ geometry with the employed boundary conditions: uniform unitary velocity in the x_2 direction on the top wall and non-slip condition ($u_1 = u_2 = 0$) at the remaining walls. For all computations, it is used a mesh with 10000 elements, with 10201 nodal points – selected in accordance with Santos *et al.* (2011).

The dimensionless parameters employed to characterize the flows are, firstly, the dimensionless flow rate U^* – also seen as the yield stress level of the fluid (see, for details, de Souza Mendes (2007)),

$$U^* = \frac{u_c}{(\dot{\gamma}_1 L_c)} \quad (7)$$

where u_c is taken as the cavity lid velocity and L_c is the cavity height. The jump number J , introduced by de Souza Mendes *et al.*, 2007, is a rheological dimensionless property for viscoplastic fluids which provides a relative measure of the shear rate jump that occurs when the stress is around the fluid yield-stress – $\tau \approx \tau_0$. Mathematically, it is defined as

$$J = \frac{\dot{\gamma}_1 - \dot{\gamma}_0}{\dot{\gamma}_0} = \frac{(\tau_0/K)^{1/n} - \tau_0/\eta_0}{(\tau_0/K)^{1/n}} = \eta_0 \left(\frac{\tau_0^{1-n}}{K} \right)^{1/n} - 1 \quad (8)$$

in which $\dot{\gamma}_0$ is the shear rate value at the beginning of the shear rate jump and $\dot{\gamma}_1$ the shear rate value for which the power-law region begins. To quantify the elastic effects on the flow, it is employed the non-dimension relaxation time, which relates the high Newtonian viscosity for very low strain rates with the below-yield relaxation time, and is defined as

$$\theta^* = \frac{\tau_0 \theta_{01}}{\eta_0} \quad (9)$$

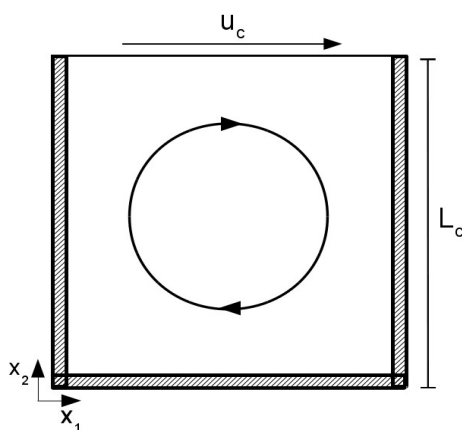
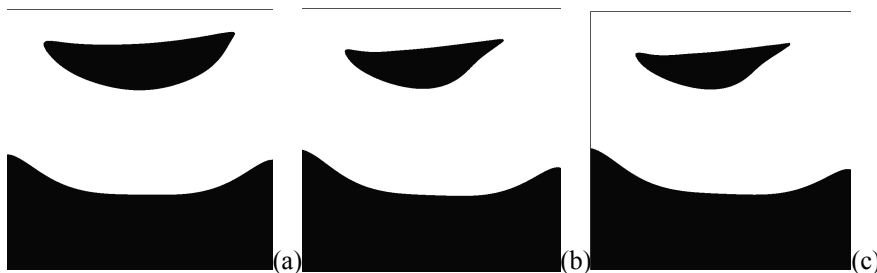


Figure 1 – The geometry.

To determine the unyielded zones of the flow, it was employed the $\dot{\gamma}_0$ -criterion, which considers unyielded the regions where the strain rate is below the strain rate at the end of the high Newtonian viscosity plateau of the viscosity function – see Santos *et al.* (2011), for details. The influence of the elasticity on the flow unyielded zones is shown on Fig. 2, ranging the non-dimensional relaxation time, θ^* , from 0.2 to 2.0, for $U^*=0.01$, $J=1000$ and $n=0.5$. We observe that with the increase of θ^* the unyielded zones (black ones at the figures) becomes asymmetric and decrease in size – once the fluid is subjected to higher stress levels.



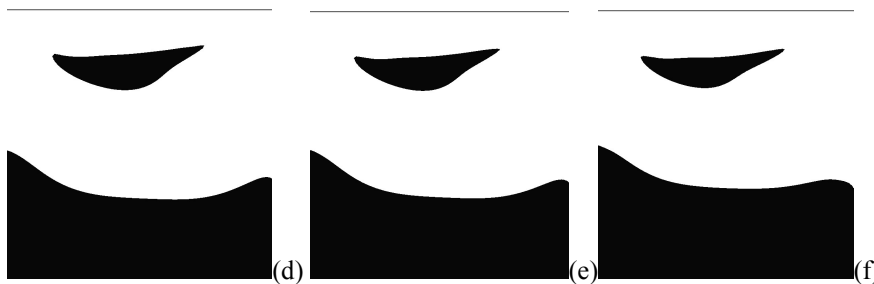


Figure 2 – Yielded and unyielded regions, for $U^*=0.01$, $J=1000$ and $n=0.5$: (a) $\theta^*=0.2$; (b) $\theta^*=0.8$; (c) $\theta^*=1.0$; (d) $\theta^*=1.3$; (e) $\theta^*=1.5$; (f) $\theta^*=2.0$.

Figure 3 show the influence of the viscosity function power-law index, varying n from 0.4 to 1.0, with $U^*=0.1$, $J=1000$ and $\theta^*=0.25$. The unyielded zones at the bottom of the cavity are slightly reduced with the increase of n – once again, higher stress levels are reached, in this case, due to the higher n indexes. The region at the center of the cavity do not present a relevant reduction/augmentation with the n variation.

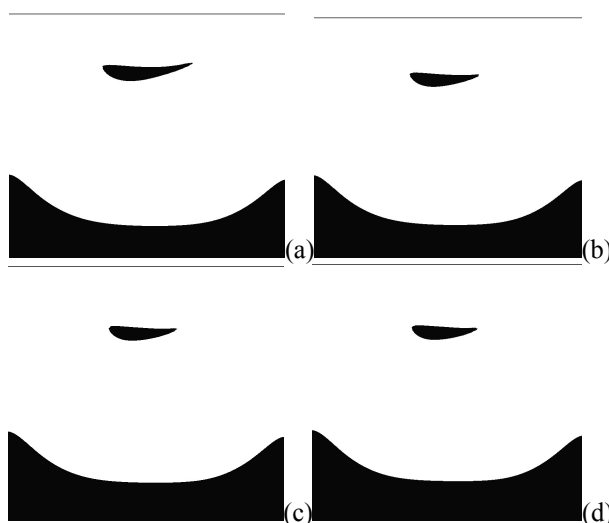


Figure 3 – Yielded and unyielded regions, for $U^*=0.1$, $J=1000$ and $\theta^*=0.25$: (a) $n=0.4$; (b) $n=0.7$; (c) $n=0.9$; (d) $n=1.0$.

The jump number variation, performed varying the η_0 viscosity, implies on the same trend observed ranging the below-yield relaxation time – once these quantities are coupled on the non-dimensional relaxation time. For low jump numbers, the unyielded regions are asymmetric, since the flow is more elastic and the stresses at the flow fields are higher. As J is increased, the unyielded zones increase and becomes symmetric.

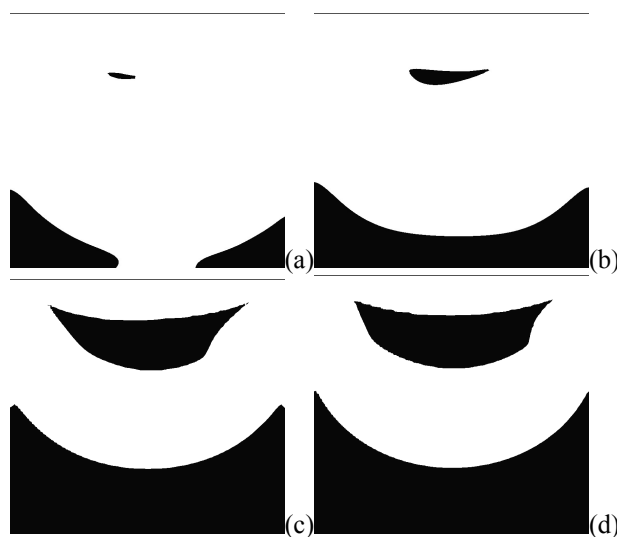


Figure 4 – Yielded and unyielded zones, for $U^*=0.1$ and $n=0.5$; and $\theta^*=0.25$: (a) $J=500$ and $\theta^*=0.5$; (b) $J=1000$ $\theta^*=0.25$; (c) $J=5000$ and $\theta^*=0.05$; (d) $J=10000$ and $\theta^*=0.025$.

4. FINAL REMARKS

In this article, some numerical simulations of inertialess flows of elasto-viscoplastic fluids have been undertaken. The elasto-viscoplastic fluid is the one introduced by Nassar *et al.* (2011) and the mechanical model is approximated via a multi-field Galerkin least-squares method in extra-stress, pressure and velocity. Due to the good stability features of the GLS method, all computations have employed a combination of equal-order bilinear Lagrangian finite elements. The numerical results have evidenced the strong influence of the non-dimension relaxation time and jump number on the size and location of the unyielded material regions. The results obtained showed a qualitatively good agreement with the related elasto-viscoplastic experimental results on literature.

5. ACKNOWLEDGEMENTS

The author D.D.O. Santos thanks the agency CAPES for his graduate scholarship and the authors S. Frey, M.F. Naccache and P.R. de Souza Mendes thanks CNPq and Petrobras for financial support.

6. REFERENCES

- de Souza Mendes, P.R., and Dutra, E.S.S., 2004, "Viscosity Function for Yield-Stress Liquids", *Applied Rheology*, Vol. 14, pp. 296-302.
- de Souza Mendes, P.R., 2007, "Dimensionless non-Newtonian fluid mechanics", *J. Non-Newt. Fluid Mech.*, Vol. 147, pp. 109-116.
- de Souza Mendes, P.R., Naccache, M.F., Vargas, P.R., Marchesini, F.H., 2007, "Flow of viscoplastic liquids through axisymmetric expansions-contractions", *J. Non-Newt. Fluid Mech.*, Vol. 142, pp. 207-217.
- Nassar, B., de Souza Mendes, P.R., Naccache, M.F., 2011, "Flow of elasto-viscoplastic liquids through an axisymmetric expansion-contraction", *J. Non-Newt. Fluid Mech.*, Vol. 166, pp. 386-394.

6. RESPONSIBILITY NOTICE

The authors are the only responsible for the printed material included in this paper.